Subregion-Specific Proteomic Signature in the Hippocampus for Recognition Processes in Adult Mice

von Ziegler, Lukas M ; Selevsek, Nathalie ; Tweedie-Cullen, Ry Y ; Kremer, Eloïse ; Mansuy, Isabelle M

Abstract: The hippocampal formation is a brain structure essential for higher-order cognitive functions. It has a complex anatomical organization and cellular composition, and hippocampal subregions have different properties and functional roles. In this study, we used SWATH-MS to determine whether the proteomes of hippocampus areas CA1 and CA3 can explain the commonalities or specificities of these subregions in basal conditions and after recognition memory. We show that the proteomes of areas CA1 and CA3 are largely different in basal conditions and that differential changes and dynamics in protein expression are induced in these areas after recognition of an object or object location. While changes are consistent across both recognition paradigms in area CA1, they are not in area CA3, suggesting distinct proteomic responses in areas CA1 and CA3 for memory formation.

DOI: https://doi.org/10.1016/j.celrep.2018.02.079

Resource

Cell Reports

Subregion-Specific Proteomic Signature in the Hippocampus for Recognition Processes in Adult Mice

Graphical Abstract

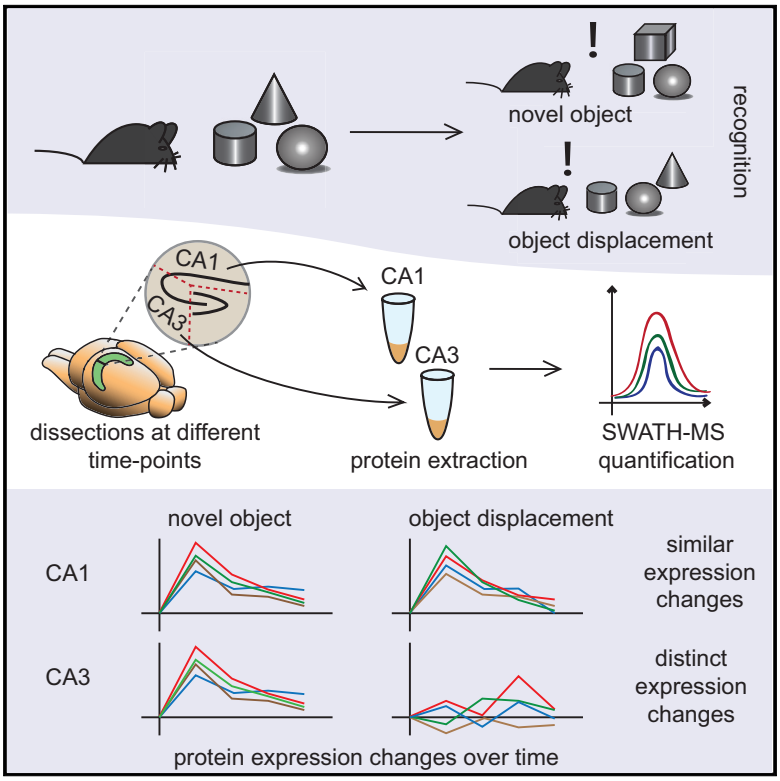

Highlights

- The proteomes of hippocampus areas CA1 and CA3 are markedly different
- But both proteomes are differentially regulated during memory formation
- The proteomic signature of area CA1 is similar for two different types of recognition memory
- The proteomic signature of area CA3 is different depending on the type of recognition memory

Authors

Lukas M. von Ziegler, Nathalie Selevsek, Ry Y. Tweedie-Cullen, Eloïse Kremer, Isabelle M. Mansuy

Correspondence

mansuy@hifo.uzh.ch

In Brief

How does the proteome differ in hippocampus areas CA1 and CA3? von Ziegler et al. identify the proteomes of areas CA1 and CA3 and characterize their dynamics during different recognition processes in adult mice.

Data and Software Availability

PXD006382

von Ziegler et al., 2018, Cell Reports *22*, 3362–3374
March 20, 2018
https://doi.org/10.1016/j.celrep.2018.02.079

CellPress

OPEN ACCESS
CellPress

Cell Reports
Resource

Subregion-Specific Proteomic Signature in the Hippocampus for Recognition Processes in Adult Mice

Lukas M. von Ziegler,[1] Nathalie Selevsek,[2] Ry Y. Tweedie-Cullen,[1] Eloïse Kremer,[1] and Isabelle M. Mansuy[1,3,*]
[1]Laboratory of Neuroepigenetics, University of Zürich/Swiss Federal Institute of Technology, Brain Research Institute, Neuroscience Center Zürich, Winterthurerstrasse 190, Zürich 8057, Switzerland
[2]Functional Genomics Center Zürich, University Zürich/Swiss Federal Institute of Technology, Winterthurerstrasse 190, Zürich 8057, Switzerland
[3]Lead Contact
*Correspondence: mansuy@hifo.uzh.ch
https://doi.org/10.1016/j.celrep.2018.02.079

SUMMARY

The hippocampal formation is a brain structure essential for higher-order cognitive functions. It has a complex anatomical organization and cellular composition, and hippocampal subregions have different properties and functional roles. In this study, we used SWATH-MS to determine whether the proteomes of hippocampus areas CA1 and CA3 can explain the commonalities or specificities of these subregions in basal conditions and after recognition memory. We show that the proteomes of areas CA1 and CA3 are largely different in basal conditions and that differential changes and dynamics in protein expression are induced in these areas after recognition of an object or object location. While changes are consistent across both recognition paradigms in area CA1, they are not in area CA3, suggesting distinct proteomic responses in areas CA1 and CA3 for memory formation.

INTRODUCTION

De novo protein synthesis is required in the brain for the formation of long-lasting memory (Squire, 2006). New proteins are needed to sustain synaptic and structural plasticity and to stabilize synaptic connections for signal transmission between neurons (Yang et al., 2009). Complex organisms have elaborate molecular systems to control protein expression. They operate by activating or inactivating gene transcription and/or translation at specific time points, allowing proper development, cellular differentiation, and functions in resting conditions and after stimulation (Molfese, 2011; Hu et al., 2012). Identifying these features is a prerequisite for a full understanding of the intimate mechanisms of memory control.

The hippocampal formation is a forebrain structure essential for learning and memory formation. Lesion studies in human and animals have demonstrated that damage to the hippocampus impairs the acquisition of information and its storage in memory. It induces severe anterograde amnesia, the inability to form new long-lasting declarative memory, in human, and it leads to learning and memory deficits in rats, mice, and monkeys (Brown et al., 2010). Electrophysiological analyses in rodents showed that certain hippocampal neurons, so-called place cells, are specifically activated when an animal is in a given location and encode spatial information (Moser et al., 2008). Place cells are also recruited to process other types of information, including olfactory and sensory signals (Eichenbaum, 2004), making the hippocampus a key structure for the perception of various forms of sensory information and the formation of different types of memory. The hippocampal formation, in particular, is required for memory for context and space. It is needed for locating and identifying objects and for navigating in an environment (Vann and Albasser, 2011). In pathological conditions, such as during social stress and depression, hippocampus-dependent memory performance involving contextual and spatial information is altered (Heckers and Konradi, 2010; Buwalda et al., 2005; Goeldner et al., 2013).

Anatomically, the hippocampal formation is a well-organized structure that comprises distinct areas, including the dentate gyrus (DG); the cornus ammonis (CA; CA1, CA2, and CA3); the entorhinal cortex; and the subiculum, which have specific structural connectivity and functional properties (Anderse et al., 2006). Although both CA1 and CA3 areas contain excitatory glutamatergic pyramidal neurons and inhibitory GABAergic interneurons, they have marked differences in connectivity and functions. CA3 pyramidal neurons can form recurrent connections with other CA3 neurons, but CA1 pyramidal neurons cannot. CA3 neurons contribute to pattern completion, the ability to map incomplete or noisy patterns to complete a full pattern. CA1 neurons are thought to match output from area CA3 with afferent, unprocessed input from the entorhinal cortex (Guzowski et al., 2004) and allow encoding of the temporal order of different contexts (Hoge and Kesner, 2007). Although many studies have examined the difference between areas CA1 and CA3 in terms of contribution to different types of memory, connectivity, and molecular characteristics, the nature of their respective proteome and its response to learning experiences have not been studied extensively. Here we demonstrate that areas CA1 and CA3 have different proteomes in the adult mouse brain, with distinct and

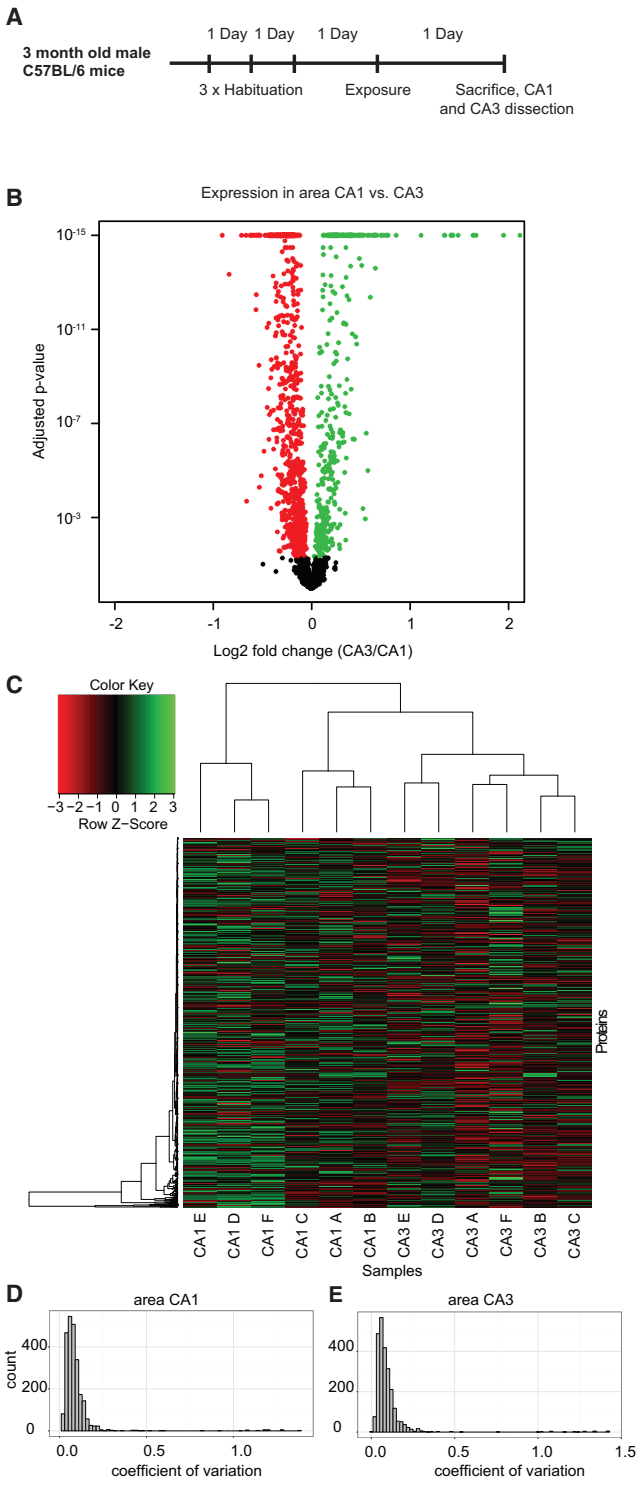

Figure 1. Differences between Proteomes in Areas CA1 and CA3 at Baseline

(A) Comparison between the proteomes of areas CA1 and CA3 in mice habituated to an arena. Animals received one habituation session per day on 3 consecutive days followed by an exposure session (initial exploration of three novel objects). Animals were sacrificed and areas CA1 and CA3 were dissected 24 hr after exposure.

(B) Volcano plot showing log2 fold change versus adjusted p value for all proteins (n = 1,697) in area CA1 (n = 6) versus CA3 (n = 6). Green proteins are significantly more highly expressed in area CA3 (BH adjusted p value < 0.05, log2 fold change [FC] cut-off 0.2, n = 189), and red proteins are significantly more highly expressed in area CA1 (n = 343).

(C) Unsupervised clustering of area CA1 and CA3 biological replicates at baseline.

(D) Histogram showing coefficients of variation for all proteins in area CA1.

(E) Histogram showing coefficients of variation for all proteins in area CA3.

See also Figures S1–S3 and Tables S1 and S2.

specific dynamics during memory formation, revealing additional properties of hippocampal subregions relevant for memory formation.

RESULTS

The Proteomes of Areas CA1 and CA3 Are Markedly Different in Basal Conditions

To determine the proteomic specificity of each hippocampal subregion, we first characterized the whole proteome in areas CA1 and CA3 in basal conditions. Basal conditions in this case are when animals are placed in the experimental arena and habituated to the arena for the same amount of time as animals used for behavioral training and testing to allow consistency across the study (Figure 1A). We used the recently developed SWATH-based proteomics technology to conduct accurate and reproducible proteome quantification (Gillet et al., 2012). SWATH-MS measurements of 6 biological replicates revealed high reproducibility, with Pearson correlation coefficients between biological replicates of 0.985–0.997 at the protein level in both areas CA1 and CA3 (Figures S1 and S2). Overall, we quantified 1,697 proteins in both areas CA1 and CA3 with two peptides or more. A statistical comparison by MSstats followed by Benjamini-Hochberg adjustment showed that 532 proteins have a different level of expression in areas CA1 and CA3 (31.3% of all proteins) (Figure 1B). Unsupervised clustering further strengthened the observation of proteome difference between areas CA1 and CA3 (Figure 1C).

Expression differences between areas CA1 and CA3 similar to mRNA differences previously described (Newrzella et al., 2007) were observed for several top-hit proteins (Figure S3). Proteins with higher expression in area CA1 in both studies included ITPKA, a regulator of inositol polyphosphates that controls morphology of hippocampal dendritic spines (Köster et al., 2016); NTM, a protein important for neurite outgrowth and adhesion (Gil et al., 1998); EFHD2, a negative regulator of nuclear factor κB (NF-κB) signaling that modulates synapse formation (Borger et al., 2014); and GAP43, a major component of growth cones associated with spine growth (Frey et al., 2000). Proteins with higher expression in area CA3 included CPNE4, a calcium-dependent phospholipid-binding protein; SYNPR, a membrane protein of small synaptic vesicles (Knaus et al., 1990); HPCAL1, a neuron-specific calcium-binding protein; and NCALD, also a neuronal calcium-binding protein. Gene ontology (GO) analyses using a web-based gene analysis toolkit (Zhang et al., 2005) on all proteins with significant differences (345 with higher expression in CA1 and 189 with higher expression in CA3) revealed increased expression of proteins related to cytoskeletal

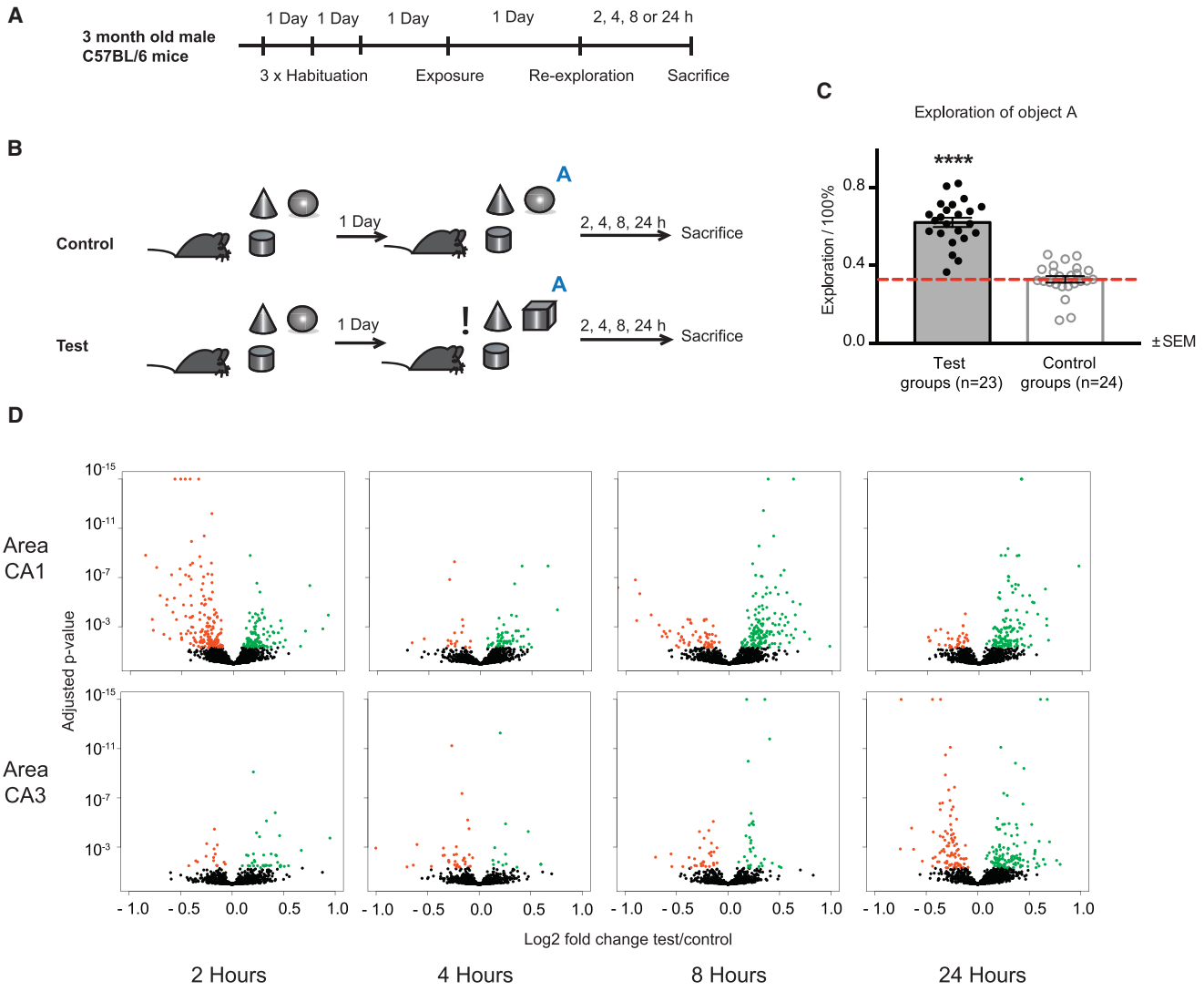

Figure 2. Changes in Protein Expression Induced by Object Recognition in Areas CA1 and CA3

(A) Experimental timeline of the OR paradigm.

(B) OR exposure and test sessions for control and test animals.

(C) Exploration of object A (unfamiliar for test animals, familiar for control animals) for test and control animals (****$p < 0.0001$). The dashed red line indicates chance level exploration of 33%.

(D) Differences in protein expression in areas CA1 and CA3 between test and control animals sacrificed after 2, 4, 8, or 24 hr. Green proteins are significantly more highly expressed (adjusted p value < 0.05), and red proteins are significantly less expressed in test versus control samples (number of animals: area CA1, 2 hr, n = 4 for each group; 4 hr, n = 4 for each group; 8 hr, n = 3 for each group; 24 hr, n = 4 for each group; area CA3, 2 hr, n = 3 for each group; 4 hr, n = 4 for each group; 8 hr, n = 4 for each group; 24 hr, n = 3 for each group).

See also Table S3.

organization in area CA1 and increased expression of proteins related to mitochondrial functions in area CA3 (Table S2). These results indicate that areas CA1 and CA3 have pronounced differences in their proteomic profile at basal conditions.

Object Recognition Induces Dynamic Changes in Protein Expression that Are Distinct in Areas CA1 and CA3

To determine how learning affects the proteome in areas CA1 and CA3, we trained mice on an object recognition (OR) task. In this task, each mouse is exposed to a set of 3 novel objects during a training session and is then tested for memory of these objects 1 day later, by being exposed to 2 of the previous objects and a novel one (Figures 2A and 2B). At testing, exploration of the novel object was higher than that of the other objects, indicating memory for the initial objects (Figure 2C). Control animals exposed to the same set of objects during training and testing explored all objects comparably at testing, suggesting equal memory for all objects. The proteome of areas CA1 and CA3 was then examined 2, 4, 8,

A

Clusters in area CA1 after object recognition

#	Cluster expression profile	Cluster significance	Enrichment in localization	Adjusted p of localization
1		36 proteins assigned 4.3 expected p = 2.1 E-21	Organelle inner membrane Mitochondrial protein complex Mitochondrial membrane part	2.55 E-7 6.9 E-6 7.35 E-6
2		47 proteins assigned 10.1 expected p = 1.7 E-17	Organelle inner membrane	2.75 E-3
3		24 proteins assigned 4.4 expecte p = 5.5 E-11	Organelle inner membrane Mitochondrial protein complex Mitochondrial membrane part	2.75 E-2 4.06 E-2 4.06 E-2
4		17 proteins assigned 3.1 expected p = 2.9 E-8	No enrichment	
5		28 proteins assigned 6.3 expected p = 1.6 E-10	No enrichment	
6		26 proteins assigned 8.6 expected p = 1.2 E-6	No enrichment	
7		21 proteins assigned 6.7 expected p = 6.6 E-6	No enrichment	
8		17 proteins assigned 4.6 expected p = 7.2 E-6	No enrichment	

B

Clusters in area CA3 after object recognition

#	Cluster expression profile	Cluster significance	Enrichment in localization	Adjusted p of localization
1		32 proteins assigned 3.5 expected p = 2.7 E-20	No enrichment	
2		32 proteins assigned 5.3 expected p = 2.4 E-15	No enrichment	
3		27 proteins assigned 6.6 expected p = 1.6 E-9	No enrichment	
4		19 proteins assigned 3.9 expected p = 3.0 E-8	No enrichment	
5		13 proteins assigned 2.8 expected p = 8.0 E-6	No enrichment	
6		21 proteins assigned 6.4 expected p = 2.2 E-10	Organelle inner membrane Mitochondrial protein complex Mitochondrial membrane part	1.71 E-12 7.57 E-3 7.57 E-3
7		14 proteins assigned 2.3 expected p = 1.8 E-7	Organelle inner membrane Mitochondrial protein complex Mitochondrial membrane part	1.36 E-3 1.36 E-3 1.36 E-3
8		12 proteins assigned 2 expected p = 1.2 E-6	No enrichment	

Figure 3. Enriched Protein Expression Profiles in Areas CA1 and CA3 following OR

(A and B) Areas CA1 (A) and CA3 (B) following OR. Profile shapes over time are shown in the left column. Other columns (from left to right) show cluster significance determined by STEM following multiple testing corrections, enrichment in localization within profiles determined by GO analyses and significance of GO analysis enrichments. See also Figure S4 and Tables S3, S4, and S5.

and 24 hr after testing and compared with that of control mice by SWATH-MS.

For areas CA1 and CA3, 1,420 and 1,366 proteins, respectively, were quantified across all time points. The expression level of multiple proteins was significantly altered in the animals exposed to a novel object at testing, in both areas CA1 and CA3 and at each time point (Figure 2D). The number of proteins with significantly changed expression and the direction of change was, however, different across time points. For area CA1, 118 proteins had an altered level of expression across several time points (3 across the 4 time points, 25 across 3 time points, and 90 across 2 time points). Further, 214 proteins were altered after 2 hr (95 upregulated and 119 downregulated), 62 proteins after 4 hr (46 upregulated and 16 downregulated), 168 proteins after 8 hr (124 upregulated and 44 downregulated), and 123 proteins after 24 hr (96 upregulated and 27 downregulated). For area CA3, 45 proteins were found to be significantly changed across several time points (2 across all 4 time points, 11 across 3 time points, and 32 across 2 time points). Further, 46 proteins had changed expression after 2 hr (11 upregulated and 35 downregulated), 39 proteins after 4 hr (27 upregulated and 12 downregulated), 43 proteins after 8 hr (22 upregulated and 21 downregulated), and 158 proteins after 24 hr (63 upregulated and 95 downregulated). Thus, in area CA1, many proteins were downregulated after 2 hr then upregulated at 8 and 24 hr. In contrast, in area CA3, the most distinct changes were only after 24 hr, and earlier time points had only small changes. These results suggest that OR alters protein expression in a time- and hippocampus subregion-specific manner.

To examine the data in a global multi-protein context, we searched for clusters of proteins with similar expression profile across time using a statistical clustering approach. Although unsupervised clustering demonstrated no strong difference between test and control across all samples (Figure S4), probably due to circadian and cage effect interferences, significant clusters of proteins could be identified in both areas CA1 and CA3 (Figures 3A and 3B) using short time expression miner (STEM) clustering. We then determined if proteins within each cluster are functionally or spatially related using GO analyses for each significant cluster. Many of the significant clusters were indeed enriched for functionality or localization. Clusters with functional enrichment were identified in both areas CA1 and CA3 with little overlap between the two. In area CA1, most clusters had a distinct downregulation after 2 hr, followed by an upregulation after 8 hr. Many of them were enriched for mitochondrial membrane and inner membrane proteins. Clusters with an opposite regulation, upregulation after 2 hr and downregulation after 8 hr, were also observed without any functional enrichment. In area CA3, clusters with upregulation at both 2 and 24 hr were observed, and they had poor functional enrichment. Another group of clusters had downregulation after 2 and 24 hr, and it was enriched for inner mitochondrial membrane proteins. Together, clustering analyses suggested three effects: (1) common profiles of protein expression are enriched in areas CA1 and CA3 after OR, (2) proteins in a given cluster (with similar expression profile) have similar enrichment in functionality or localization, and (3) areas CA1 and CA3 have distinct protein clusters and dynamics after OR.

Object Location Recognition and OR Alter Protein Expression in Areas CA1 and CA3 Differently

To investigate if protein expression in areas CA1 and CA3 is changed in a common or task-specific manner, we repeated the experiments using a second learning paradigm related to OR but different, an object location recognition (OLR) task (Figure 4A). In this task, animals have to remember the location of

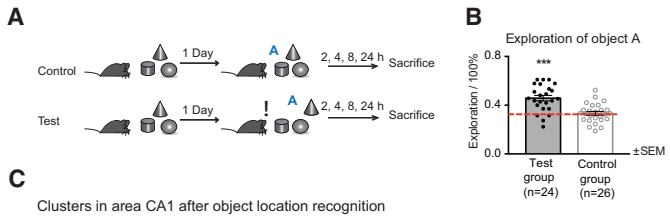

C

Clusters in area CA1 after object location recognition

#	Cluster expression profile	Cluster significance	Enrichment in localization	Adjusted p of localization
1		20 proteins assigned 2.6 expected p = 5.4 E-12	Organelle inner membrane Mitochondrial protein complex Mitochondrial membrane part	2.63 E-5 1.66 E-4 8.73 E-4
2		23 proteins assigned 4.4 expected p = 2.5 E-10	Organelle inner membrane Mitochondrial protein complex Mitochondrial membrane part	8.46 E-6 9.22 E-4 1.13 E-3
3		18 proteins assigned 4.2 expected p = 4.2 E-7	No enrichment	

D

Clusters in area CA3 after object location recognition

#	Cluster expression profile	Cluster significance	Enrichment in localization	Adjusted p of localization
1		43 proteins assigned 8 expected p = 9.9 E-19	vesicle membrane transport vesicle presynapse	5.67 E-4 4.02 E-2 4.02 E-2
2		25 proteins assigned 3.3 expected p = 1.2 E-14	No enrichment	
3		13 proteins assigned 1.5 expected p = 7.7 E-9	No enrichment	
4		13 proteins assigned 1.9 expected p = 8.9 E-8	No enrichment	
5		10 proteins assigned 1.3 expected p = 9.3 E-7	No enrichment	
6		24 proteins assigned 4.9 expected p = 3.6 E-10	No enrichment	
7		15 proteins assigned 1.8 expected p = 6.6 E-10	No enrichment	

Figure 4. Changes in Protein Expression Induced by OLR in Areas CA1 and CA3

(A) OR exposure and test sessions for control and test animals

(B) Exploration of object A (displaced for test animals, not displaced for control animals) for test and control animals (***$p < 0.001$). The dashed red line indicates chance level exploration of 33%.

(C and D) Enriched protein expression profiles in areas CA1 (C) and CA3 (D) following OLR. Profile shapes over time are shown in the left column. Other columns (from left to right) show cluster significance determined by STEM following multiple testing corrections, enrichment in localization within profiles determined by GO analyses and significance of GO analysis enrichments (number of animals: area CA1, 2 hr, n = 4 for each group; 4 hr, n = 4 for each group; 8 hr, n = 4 for control and n = 3 for test; 24 hr, n = 4 for each group; area CA3, 2 hr, n = 4 for each group; 4 hr, n = 4 for each group; 8 hr, n = 4 for each group; 24 hr, n = 4 for each group). See also Figure S5 and Tables S3, S4, and S5.

an object (tested by displacing the object and assessing exploration after displacement) in an arena containing three familiar objects. OLR is known to specifically recruit hippocampal functions, while OR relies also on cortical structures. Changes in protein expression across time were examined as with OR by SWATH-MS followed by statistical clustering. Again, significant clusters of proteins in both areas CA1 and CA3 could be detected (Figures 4C and 4D; unsupervised clustering, Figure S5). In area CA1, clusters with downregulation after 2 hr and upregulation after 8 hr and enriched for mitochondrial inner membrane proteins were observed, similarly as in the OR paradigm. However, in area CA3, only clusters with a distinct upregulation after 4 hr and enriched for vesicle and pre-synaptic protein were detected. These results suggest that OLR induces changes in protein expression in a time- and hippocampus subregion-specific manner.

Changes in Protein Expression after OR and OLR Correlate in Area CA1, but Not in Area CA3

To assess the correlation between OR and OLR paradigms, we compared the expression patterns of protein clusters across the 2 paradigms (Figures 5A and 5B). Comparing cross-correlations between datasets revealed decreased p values for clusters observed in both OR and OLR in area CA1 (Figure 5C). In contrast, there was no increase in correlation in area CA3 between the two paradigms, or between areas CA1 and CA3 within paradigms, when compared with randomized data (Figure 5D). Overall, these analyses thus revealed that (1) changes in protein expression induced by training are different in areas CA1 and CA3, (2) changes in area CA1 correlate in both OR and OLR tasks, and (3) changes in area CA3 do not correlate between OR and OLR tasks. These results suggest that, proteome-wise, area CA1 contributes to OR and OLR in a similar manner, while area CA3 contributes differently.

Electron Transport Chain Proteins Are Selectively Regulated in Area CA1 following OR and OLR

To gain functional insight into the proteins activated in the clusters, we searched for proteins enriched in area CA1 after both OR or OLR. Many of the proteins within these clusters are located in the inner mitochondrial membrane, and they are components of the electron transport chain (ETC). Notably, all ETC proteins assigned to significant clusters had similar dynamics: they were downregulated after 2 hr and then upregulated after 8 hr (Figure 6A). Upregulation after 8 hr was validated for ATP5A with new biological replicates, including a third no re-exposure control group, confirming an OR-specific effect of ATP5A (Figure S6). Correlation analyses of all quantifiable ETC proteins revealed a strong correlation between OR and OLR in area CA1, but not in area CA3 (Figures 6B and 6C). Further, comparing ETC proteins with other mitochondrial proteins showed that changes are specific for ETC proteins and do not affect other mitochondrial proteins (Figure 6D).

DISCUSSION

This study provides evidence that different forms of learning activate different and specific proteomes in hippocampus areas

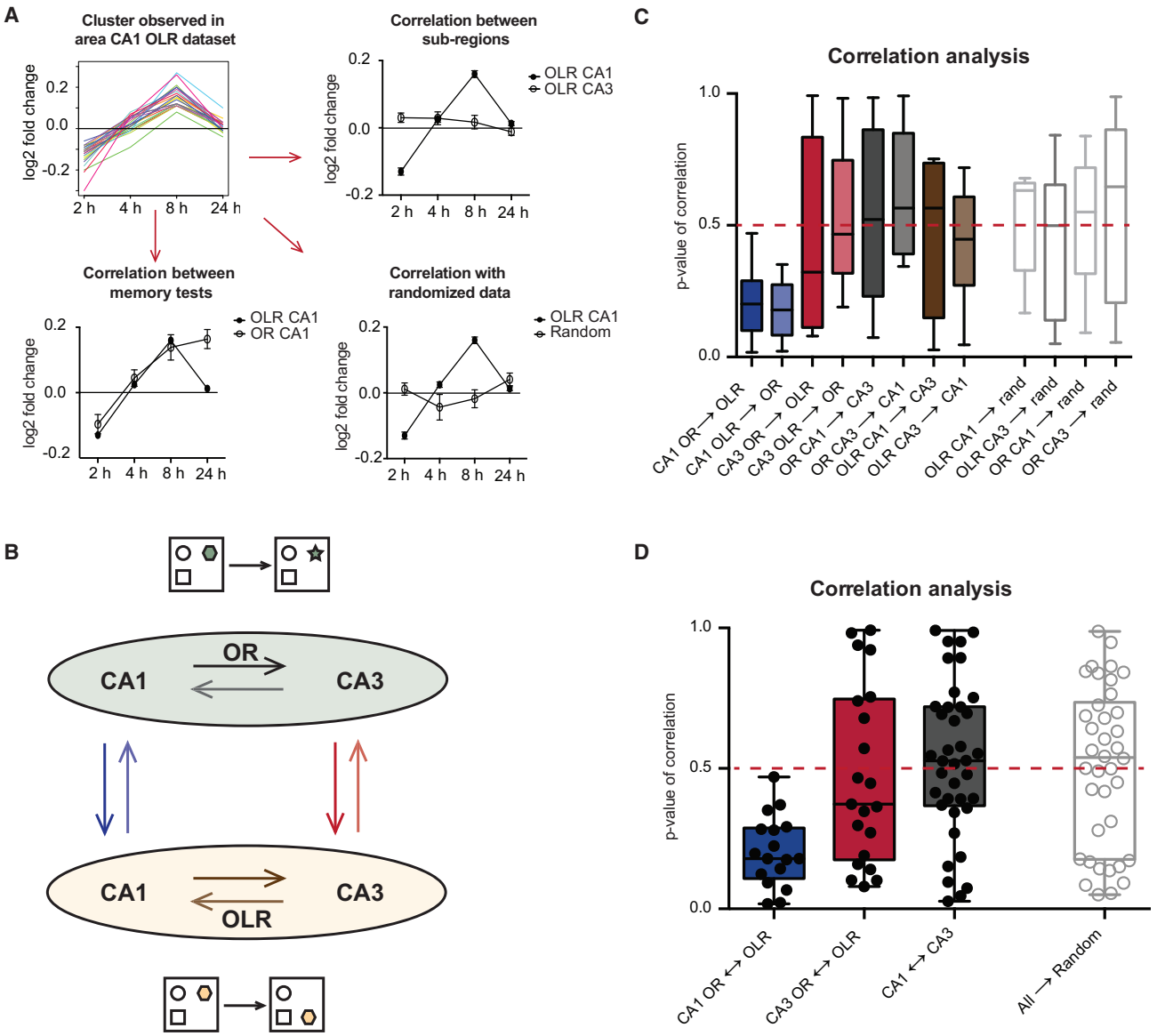

Figure 5. Correlation of Changes in Protein Expression between OR and OLR and Areas CA1 and CA3

(A) Correlation analyses for one illustrative cluster. Top left: expression change data of all proteins within this cluster in the OLR paradigm in area CA1 between control and test at each time point. Top right: expression change of the same proteins in OLR area CA1 and OLR area CA3 shows correlation between subregions for these proteins. Bottom left: expression change of the same proteins in OLR area CA1 and OR area CA1 shows correlation between memory tests for these proteins. Bottom right: correlation with a randomized dataset is shown (random re-assignment of fold changes within the experiment).

(B) Illustration of analyzed correlations between OR and OLR and between areas CA1 and CA3.

(C) p values of correlation for comparisons in (B) (Kruksal-Wallis p value = 0.0249, column statistics with Wilcoxon signed-rank test and hypothetical mean of 0.5: CA1 OR → OLR, p = 0.0005; CA1 OLR → OR, p = 0.0625) show increased correlation within area CA1 between learning paradigms. Colors of boxes correspond to colors of arrows in (B).

(D) Pooled data for (C) combining CA1 OR versus OLR correlations (blue in B), CA3 OR versus OLR correlations (red in B), correlations of CA1 versus CA3 in both paradigms (gray and brown in B), and all correlations with randomized data (white in B) (Kruksal-Wallis p value = 0.0008, column statistics with Wilcoxon signed-rank test and hypothetical mean of 0.5: CA1 OR ↔ OLR, p < 0.0001; all others nonsignificant [ns])

CA1 and CA3. It shows that recognition of an object or recognition of an object location induces large changes in protein expression that distinguish areas CA1 and CA3 and are dynamically regulated differently in these areas across time. It identifies clusters of proteins within a subregion that are enriched for functions and cellular distribution and have similar expression profiles on both tasks. Comparing the type, expression pattern, and temporal regulation of proteins represented in each cluster reveals a strong correlation between OR and OLR paradigms in area CA1, but not in area CA3, suggesting striking differences

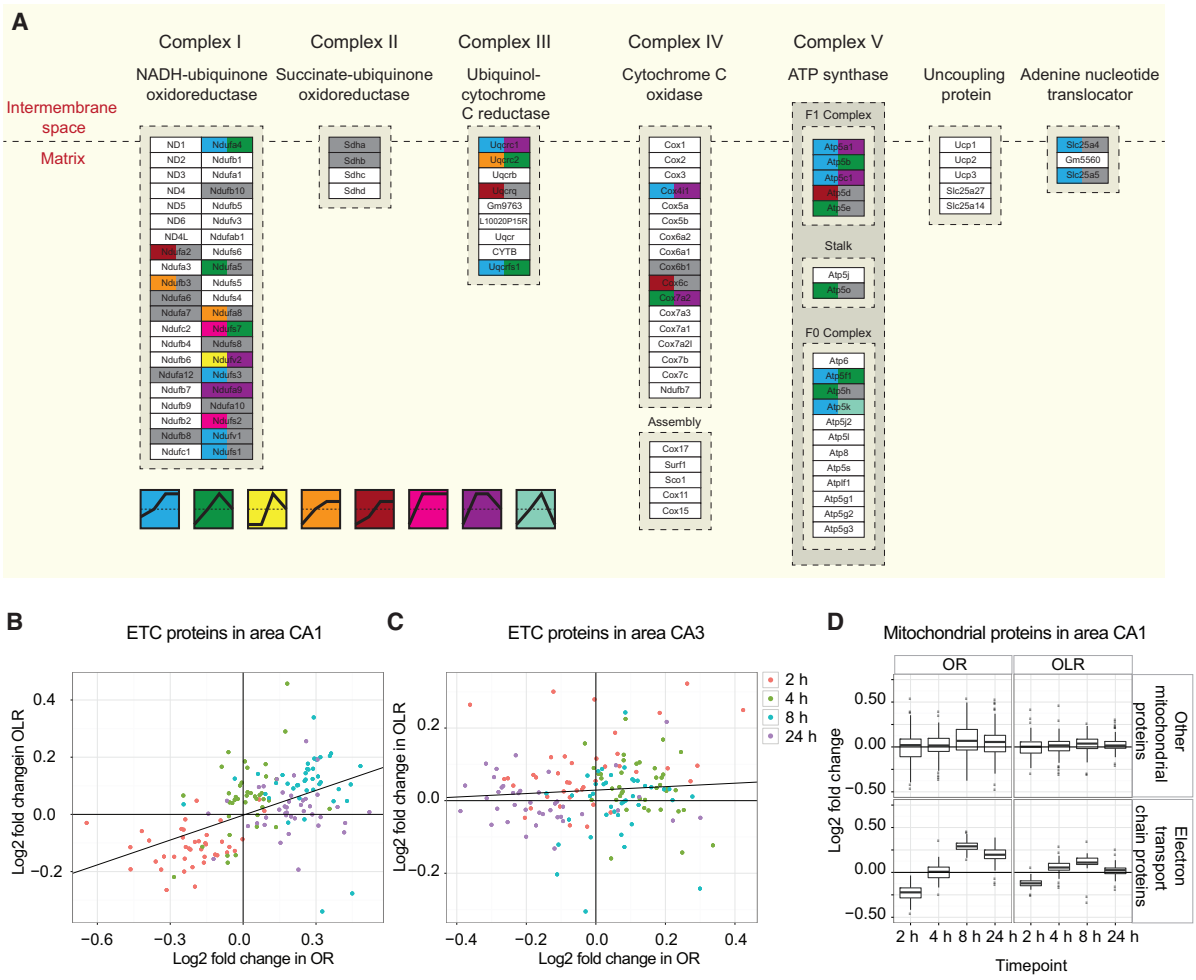

Figure 6. Changes in Electron Transport Chain Proteins following OR and OLR

(A) Expression profile of ETC proteins in area CA1 following OR and OLR. White protein boxes indicate proteins that could not be quantified. Color on the left side of protein boxes indicates their expression profile in the OR paradigm, and color on the right side indicates expression profile in the OLR paradigm. All significant profiles that any of the ETC proteins followed are shown. Gray indicates proteins that did not follow any of the colored profiles.

(B) Linear regression model of all quantifiable ETC protein log2 fold changes between OR and OLR in area CA1. Colors indicate time points. Linear model statistics: log2OR = 0.29 * log2OLR, p value of slope = $3.19*10^{-12}$, $R^2 = 0.27$.

(C) Linear regression model of all quantifiable ETC protein fold changes between OR and OLR in area CA3 shows no significant correlation.

(D) Boxplot displaying log2 fold changes of ETC protein and all other mitochondrial proteins in area CA1 following both OR and OLR.

See also Figure S6.

between the proteomes of areas CA1 and CA3 relevant for memory formation. The results of this study, however, should be interpreted with caution, since resolving cell type-specific effects from whole hippocampus extracts is not possible. The ratio of neurons to glial cells in the hippocampus is roughly 1:2 while volumetric ratio is around 1:1 (Oliveira-da-Silva et al., 2009); observed changes could arise from either one, or both, of these cell populations.

Few studies have looked at memory-dependent changes in protein expression in the hippocampus, and ours is notable because it describes CA1- and CA3-specific effects in detail. A recent report examined protein expression changes in the whole hippocampus following a spatial memory task (radial arm maze) over multiple days (Borovok et al., 2016), and it identified proteins with altered expression during the memory acquisition phase (day 1), the steep learning improvement phase (day 3), and the final curve of the learning phase (day 5). While yielding interesting results, including changes in proteins associated with mitochondrial metabolism activity, this study analyzed protein expression following multiple consecutive learning experiences, and it used naive home cage mice as a control group, making it impossible to distinguish between learning-induced effects and effects induced by exploration and increased activity. Additionally, the time points cover long-term effects, but short- or medium-term effects on the order of hours following learning are not described.

Another study has examined the temporal protein expression profile in rat DG during memory consolidation following water

maze training using 2D-DIGE (two dimensional-difference gel electrophoresis) followed by excision of significantly altered spots and characterization with mass spectrometry (MS) (Monopoli et al., 2011). This study demonstrated changes over a 1-day period at multiple time points (3, 6, 12, and 24 hr) that encompass both medium-term and long-term effects, with enrichments for cellular structure components and proteins involved in cellular metabolism. Animals in this study were sacrificed at their corresponding time point with only one control group, making it difficult to control for circadian effects. Another study analyzed the effect of fear conditioning on hippocampal protein expression in the synaptic membrane (Rao-Ruiz et al., 2015). It used a delayed-shock group for memory formation and an immediate-shock group as a stress control, and it analyzed protein expression using isobaric tags for relative and absolute quantitation (iTRAQ) after 1 and 4 hr. It reported no change in protein expression following 1 hr but extensive changes after 4 hr. A direct comparison between these studies and ours is, however, difficult due to differences between paradigms, time points, and experimental design.

The hippocampus is a key brain structure for cognitive processes that allows the formation of episodic memory and the detection of novelty. The formation of episodic memory requires the encoding of contexts and information encountered at a given time, as well as the encoding of the temporal relationship of the different contexts, for instance the order in which they were encountered. The detection of novelty by the hippocampus involves the recall of stored memories about context and the identification of match/mismatch with the newly encountered context. Areas CA1 and CA3 contribute differently to these processes. While area CA1 is necessary for the detection of novelty (Lisman and Otmakhova, 2001) and the encoding of the temporal order of contexts (Huerta et al., 2000; Gilbert et al., 2001; Hoge and Kesner, 2007; Hunsaker et al., 2008; Kesner et al., 2010), area CA3 is required for the encoding of the context itself (Leutgeb et al., 2004; Rajji et al., 2006). Both OR and OLR have been shown to depend mainly on hippocampal functions (Cohen and Stackman, 2015). While some studies have argued that OR is independent of hippocampal functions (Lee et al., 2005), they relied on multiple exposures to the same objects, a process that induces familiarity. Familiarity in contrast to recall is a semantic form of memory, which is independent of recollection of details associated with the objects and does not require hippocampal functions (Yonelinas et al., 2002). For a single exposure, OR has been shown to rely on the hippocampus (Broadbent et al., 2009). Interestingly, in our data, the overall expression change response following OR is stronger than following OLR, which could be explained by a stronger overall activation of the hippocampus during the OR paradigm.

Our results identify a pool of proteins whose expression is changed in area CA1 after these two behavioral tasks that rely upon the detection of novelty, novelty for an object in OR, and novelty for an object location in OLR. These proteomic changes are likely associated with the detection of novelty because they are not induced when the same object or the same object location is presented. They may be necessary for the formation of new episodic memory. In contrast to area CA1, changes in protein expression in area CA3 are different after OR and OLR. While only a few proteins are changed following OR, many proteins, in particular synaptic proteins, are upregulated 4 hr after OLR. This suggests that different processes are engaged in area CA3 after OR and OLR that may depend on the type of novelty. This is consistent with the role that area CA3 plays in the encoding of context, which, in the OLR paradigm, involves a change in location (spatial configuration) of an object. It has been proposed that a context can have both spatial and non-spatial components and that spatial components are encoded first to generate a scaffold for representation of the whole context. Non-spatial cues are then added to this scaffold in subsequent steps (Knierim et al., 2006). This implies that alteration of spatial features of a context, like that occurring in OLR, but not in OR, would require either the remodeling of an existing neural representation of the context or the formation of a new representation. Such a process would likely rely on plasticity within area CA3, a process that may require *de novo* protein synthesis (Cajigas et al., 2010) as exemplified by the changes in synaptic proteins observed in our proteomic analyses.

Another feature of our data is the temporal alteration of the expression of ETC proteins in area CA1 following both, OR and OLR. It cannot be concluded if these changes happen uniformly in the tissue, in neurons or glial cells exclusively, or even in only a sub-set of neurons or glial cells, i.e. activated neurons. However, neurons have a high mitochondrial density, rely heavily on mitochondria to maintain homeostasis, and use up to 96% of all ATP produced in gray matter (Zhu et al., 2012), so we can assume that most of the observed changes represent alterations in neurons. Both CA1 and CA3 contain glutamatergic excitatory neurons (~90% of the total neuron population) as well as GABAergic inhibitory interneurons (~10% of the total neuron population), but an interneuron-specific effect is unlikely since it would have to be very large to explain the overall observed effect.

The alterations in ETC proteins could be induced by the detection of novelty, and they could contribute to neuronal activity necessary for the formation of episodic memory. The recognition of novelty in OR and OLR has been associated with activity changes in area CA1, but not in area CA3 (Larkin et al., 2014); it increases the activity of excitatory CA1 pyramidal neurons but decreases the activity of inhibitory CA1 interneurons (Wilson and McNaughton, 1993; Nitz and McNaughton, 2004; Csicsvari et al., 2007; Karlsson and Frank, 2008; VanElzakker et al., 2008). Neurons in area CA1 are not only more readily activated but their increased excitability lasts longer (Moyer et al., 1996; McKay et al., 2009). The increased excitability could result from higher intracellular ATP, which, in neurons, attenuates K_{ATP} channels, favors membrane depolarization, and shifts cells into a more excitable state (Huang et al., 2007). ATP itself is produced at the inner mitochondrial membrane by ETC via oxidative phosphorylation. Thus, the increase in ETC proteins observed in area CA1, but not in area CA3, may elevate neuronal ATP production 8 and 24 hr after training and, thereby, sustain persistent excitability specifically in these neurons. This may ultimately help the formation of episodic memory, since increased excitability in area CA1 has been shown to be linked to episodic memory formation (Cai et al., 2016). The ensemble of neurons in area CA1 that are activated during contextual tasks have increased

excitability so as to facilitate the concurrent encoding of other contextual memories occurring within close temporal proximity. Several studies have confirmed that area CA1 is key to forming temporal associations between different contexts (Huerta et al., 2000; Gilbert et al., 2001; Hoge and Kesner, 2007; Hunsaker et al., 2008; Kesner et al., 2010).

Multiple links between ETC proteins and memory formation have previously been reported in aging and pathological conditions. Decreased excitability of CA1 pyramidal neurons was demonstrated in aged mice and contributes to aging-related cognitive impairments (Oh et al., 2010, 2016; Kaczorowski and Disterhoft, 2009). Aging-related mitochondrial dysfunctions, including reduced ETC efficiency, have also been described in mice (Navarro and Boveris, 2010; Navarro et al., 2008), providing a link between ETC functions and aging-related decrease of area CA1 neuron excitability. Similar mitochondrial dysfunctions have also been observed in neurodegenerative disorders characterized by cognitive impairment, such as Alzheimer's disease (Maruszak and Żekanowski, 2011), Parkinson's disease (Winklhofer and Haass, 2010), traumatic stress (Zhang et al., 2006), major depressive disorder (Tobe, 2013), and hypoxia (Solaini et al., 2010).

Intriguingly, while ETC proteins were increased 8 and 24 hr after novelty detection, they were decreased 2 hr after, suggesting dynamic regulation of these proteins and different functions in the short and long term. Although an increased and prolonged excitability of CA1 neurons could help memory formation, it may also make neurons more susceptible to oxidative damage, in particular, following periods of high activity. Oxidative damage occurs when the production of reactive oxygen species (ROS) is excessive and cannot be overcome by the ability of the cell to chemically deactivate them through reduction. Most ROS are produced in mitochondria, predominantly in complexes I and III of the ETC, and they are present as a natural by-product of cellular metabolism (Lambert and Brand, 2009). Neuronal stimulation through NMDA receptors increases ROS production and overstimulation can damage neurons and lead to excitotoxic cell death (Girouard et al., 2009; Gunasekar et al., 1995). Downregulation of ETC proteins in area CA1 2 hr after training may be a protective mechanism to prevent oxidative damage following a period of increased activity. Such downregulation could occur by directed degradation of ETC proteins through the ubiquitin-proteasome system (UPS), shown to control multiple aspects of mitochondrial functions (Franz et al., 2015). It can selectively tag proteins by conjugation with ubiquitin followed by degradation (Nandi et al., 2006). Many inner mitochondrial proteins can be conjugated to ubiquitin, and ubiquitin system components localize to mitochondria (Lehmann et al., 2016), allowing the UPS to potentially function within mitochondria.

The present data therefore suggest that a dynamic system through which ETC proteins are temporally regulated may have a key role in balancing cell excitability within area CA1 of the hippocampus. Impairments in this system could contribute to pathologies characterized by abnormalities in ETC expression. A better understanding of the dynamics and regulation of ETC proteins could provide the basis of novel therapeutic approaches in these pathologies.

EXPERIMENTAL PROCEDURES

Animal Care and Housing

Care of animals and all protocols conformed to the guidelines of the Veterinary Office of the Canton of Zurich, Switzerland, and they were approved by the Commission for Animal Research (licenses 54/2012 and 41/2015). Adult (2- to 3-month-old) wild-type male C57BL/6 mice were maintained in a temperature- and humidity-controlled facility on a 12-hr-reversed light/dark cycle, with food and water *ad libitum* in cages of 3–5 animals. Subjects were euthanized by cervical dislocation.

OR and OLR Paradigms

OR and OLR were used to induce memory for objects or object location in adult (2- to 3-month-old) wild-type C57BL/6 male mice. Animals were habituated to an empty arena (square box with plexiglas walls, 40 × 40 × 40 cm) in a dimly lit room. Each animal was allowed to explore the arena individually for 5 min. Habituation was repeated daily on 3 consecutive days. For training, animals were placed in the arena containing three different unfamiliar objects located on 3 of the 4 corners of a virtual square in the center (20 × 20 cm) of the arena. The animals explored the set of objects for 15 min. Exploration of the objects was recorded with an infrared camera and analyzed with a video-tracking system (Viewpoint Behavior Technology, Lyon, France). Animals were returned to their home cage for 24 hr before testing. In OR, animals were tested with two of the initial objects and a novel object (unfamiliar to the animals) for 15 min. In OLR, animals were tested with the three familiar objects but one was spatially displaced (moved to the empty corner of the square in the center) for 15 min. Control animals were tested with the same objects at the same place. Exploration of objects was also tracked manually using Labwatcher (Viewpoint Behavior Technology, Lyon, France). Animals were sacrificed 2, 4, 8, or 24 hr after testing.

Experimental Design

Animals from the same cage were evenly distributed to test and control groups for each time point (2, 4, 8, and 24 hr). Behavioral testing was conducted in successive sessions, each session with 6 test and 6 control animals at a given time point. Behavioral sessions always started at the same time of the day (11:00 a.m.). A block design was used to reduce bias from samples processing or measurement. For this, samples were divided into multiple blocks, with each block containing one sample of each group (test and control) at each time point. The order in which blocks were processed and measured was randomized. The sample order within blocks was first randomized for sample processing (protein extraction, protein digestion, and peptidic cleanup) and then re-randomized for SWATH-MS measurements.

Dissection of Areas CA1 and CA3

Animals were killed by cervical dislocation followed by decapitation. The brain was isolated in a tray of ice-cold PBS buffer and transferred to filter paper for dissecting the hippocampus. Filter papers were cooled with PBS-ice to prevent tissue warming. Isolated hippocampi were transferred to a binocular microscope and cooled with PBS-ice. Area CA3 was dissected by cutting along the minor hippocampal fissure along the dorsoventral axis of the hippocampus. Area CA1 and DG were separated with a pincer and incision scalpel by gently pushing the blade along the major hippocampal fissure. Areas CA1 and CA3 were snap-frozen in liquid nitrogen and stored at −80°C until further processing.

Protein Extraction and Digestion

Proteins were extracted and processed for SWATH-MS analyses. Proteins were extracted from areas CA1 and CA3 samples using 200 μL TEAB buffer (100 mM triethylammonium bicarbonate, 0.1% SDS, 1:100 protease inhibitor cocktail P8340 [Sigma-Aldrich, St. Louis, MO, USA], and 1:500 PMSF [50 mM in EtOH]). The samples were mechanically lysed by 15 strokes with a 26G needle and sonicated for 2 min. Samples were spun down at 16,000 × *g* for 30 min at 4°C and supernatants were collected. Proteins were quantified using a Qubit protein assay kit (Thermo Fisher Scientific, Waltham, MA, USA) following the manufacturer's protocol. Protein extracts were further processed with a filter-assisted sample preparation protocol

(Wiśniewski et al., 2009). 20 μg protein was filled up to 30 μL final volume with SDS denaturation buffer (4% SDS [w/v], 100 mM Tris/HCL [pH 8.2], and 0.1 M DTT). For denaturation, samples were incubated at 95°C for 5 min. Samples were diluted with 200 μL UA buffer (8 M urea and 100 mM Tris/HCl [pH 8.2]) and then loaded to regenerated cellulose centrifugal filter units (Microcon 30, Merck Millipore, Billerica, MA, USA). Samples were spun at 14,000 × *g* at 35°C for 20 min. Filter units were washed once with 200 μL UA buffer followed by centrifugation at 14,000 × *g* at 35°C for 20 min. Cysteines were blocked with 100 μL IAA solution (0.05 M iodoacetamide in UA buffer) for 1 min at room temperature in a thermomixer at 600 rpm, followed by centrifugation at 14,000 × *g* at 35°C for 15 min. Filter units were washed 3 times with 100 μL UA buffer and then twice with a 0.5-M NaCl solution in water (each washing was followed by centrifugation at 35°C and 14,000 × *g* for 15 min). Proteins were digested overnight at room temperature with a 1:50 ratio of trypsin (0.4 μg) in 130 μL TEAB (0.05 M Triethylammoniumbicarbonate in water). After protein digestion, peptide solutions were spun down at 14,000 × *g* at 35°C for 15 min and acidified with 3 μL 20% TFA (trifluoroacetic acid).

Western Blotting

20 μg protein was denatured with 4× Laemmli Sample Buffer (Bio-Rad, Hercules, CA, USA) and 10% of mercaptoethanol for 5 min at 95°C, loaded onto 4%–20% gradient Mini-PROTEAN TGX gel (Bio-Rad, Hercules, CA, USA), and separated at 70 V for 30 min and then 170 V for 1 hr using SDS running buffer (25 mM Tris, 192 mM Glycin, and 0.1% SDS). Proteins were transferred using a Trans-BlotTurboBlotting System and a Trans-BlotTurboMini Nitrocellulose transfer pack (both Bio-Rad, Hercules, CA, USA) for 7 min at 2.5 A. Membranes were blocked using 5% of non-fat dry milk for 1 hr at room temperature (RT), and they were incubated overnight with 5 mL 1:5,000 anti-ATP5A (ab118482, Abcam, Cambridge, UK) at 4°C, for 1 hr at RT with 5 mL 1:2,500 anti-GAPDH (14C10, Cell Signaling Technology, Danvers, MA, USA) and for 1 hr at RT with 1:10,000 IRDye 800CW anti-Rabbit IgG (926-32211, LI-COR, Lincoln, NE, USA). Between incubations, membranes were washed with TBS-Tween 3 times for 10 min each. Membranes were imaged using an Odyssey Infrared Imaging System (LI-COR, Lincoln, NE, USA) and quantified using ImageJ (version [v.]1.41).

Hydrophobic Interaction Liquid Chromatography for Peptide Fractionation

HILIC (hydrophobic interaction liquid chromatography) was used to fractionate peptides from whole hippocampus protein extracts in order to prepare a broader spectral library. The trypsinated sample was filled up to a final volume of 1.3 mL 75% acetonitrile (ACN) and 10 mM KH_2PO_4. 5 μL 50% phosphoric acid was added to ensure a pH of 4.5. The sample was fractionated using an 1100 series HPLC system (Agilent Technologies, Santa Clara, CA, USA) into 9 separate fractions.

Peptide Cleanup

Peptides were cleaned up using Sep-Pak C18 silica columns (Waters, Milford, MA, USA). Columns were activated with 1 mL methanol and washed with 1 mL 60% ACN and 0.1% TFA. Columns were equilibrated with 3 × 1 mL 3% ACN 0.1% TFA. Samples were diluted in 800 μL 3% ACN 0.1% TFA and loaded onto the columns. They were then washed with 4× 1 mL 3% ACN 0.1% TFA and eluted with 60% ACN 0.1% TFA. Samples were lyophilized in a speedvac and then re-solubilized in 19 μL 3% ACN 0.1% FA (formic acid) prior to measurement. 1 μL synthetic peptides (Biognosys, Switzerland) was added to each sample for retention time calibration.

SWATH-MS Measurements

Samples were measured on a TripleTOF 5600 (SCIEX, Framingham, MA, USA) in SWATH mode using a previously described method (Gillet et al., 2012). Peptides were separated with an Eksigent NanoLC (SCIEX, Framingham, MA, USA). Each sample (4 μL) was injected and loaded onto a 1.8-μm, 100-Å C18 column (heated to 50°C). Peptides were separated using a 144-min linear solvent gradient of 3%–40% ACN. Fixed 25-Da precursor isolation windows were used within a precursor range of 300–1,200 m/z. Fragment ions were acquired in a range of 200–1,800 m/z.

Shotgun Measurements

To generate an extensive tissue-specific spectral library, samples from the SWATH-MS sample pool and fractions from pre-fractioned hippocampus sample were used for shotgun measurements. 8 samples from the sample pool of both OR and OLR experiments were chosen randomly. Additionally, all nine HILIC fractions from whole hippocampus extracts were individually measured. Measurements were performed on a TripleTOF 5600 System (SCIEX, Framingham, MA, USA) as for SWATH-MS measurements. Peptides were separated with an Eksigent NanoLC (SCIEX, Framingham, MA, USA). Each sample (4 μL) was injected and loaded onto a 1.8-μm, 100-Å C18 column (heated to 50°C). Peptides were separated using a 144-min-long linear solvent gradient of 3%–40% ACN. MS1 was acquired in a 300- to 1,200-m/z range, and MS2 was acquired in a 200- to 1,800-m/z range.

MS/MS Ion Searches of Shotgun Measurements

MASCOT (Matrix Science, London, England) was used for MS/MS ion searches. For each shotgun run a Mascot search file was generated. Mascot search files from all shotgun runs were merged into a single search file using mascot daemon (Matrix Science, London, England). The merge file was searched against a tryptic digestion of a decoyed mouse proteome (UniProt: 10090). Carbamidomethyl at cysteine was assumed as fixed modification and oxidation of methionine as variable modification. No missed cleavages were allowed. A peptide mass tolerance of ±20 ppm and a fragment mass tolerance of ±0.1 Da were used.

Generation of a Spectral Library and a Precursor-iRT List

DAT files from MS/MS ion searches were exported with Mascot and loaded into Skyline (MacCoss Lab) to generate a spectral library with a false discovery rate of 1%. Libraries were generated with single entries for every precursor, choosing the ones with the best mascot scores if multiple spectra were available. Retention times of spiked-in indexed retention time (iRT)-peptides (Biognosys, Switzerland) from all shotgun MS runs were manually exported and used to generate an iRT-versus-retention time linear regression for every run. These regressions were then used to calculate iRT values for all spectral library entries from the measured retention times of the corresponding MS runs. Using this approach, a precursor list with corrected iRT values for the whole proteome was generated.

Generation of a Spectronaut Assay List

The precursor-iRT list and the spectral library were used to generate an assay list for Spectronaut (v. 6, Biognosys, Switzerland). The whole mouse proteome from UniProt (UniProt: 10090) was loaded into Skyline, and an *in silico* digestion using trypsin with a KR|P cutting profile without allowing for any missed cleavage was performed. Peptides with a minimum length of 8 and a maximum length of 25 were included, and 25 N-terminal amino acids were excluded. Carbamidomethyl was assumed as a fixed modification for cysteine. Precursor charges of 2+ or 3+ and ion charges of 1+ or 2+ for all ion types (x, y, z, a, b, and c) were included. For each precursor, the 4 fragment ions with the highest intensity within an m/z range of 200–1,800 in the spectral library were selected and exported as an assay list compatible with Spectronaut (v. 6, Biognosys, Switzerland). Correct iRT values were added to the assay list by comparison with the precursor-iRT list.

SWATH-MS Transition Identification and Quantification

For identification and quantification of transitions in SWATH-MS data (Gillet et al., 2012), automated peak picking was used. The previously prepared assay list was used to define transitions, relative intensities, and iRT values. Spectronaut (v. 6, Biognosys, Switzerland) was used for automated peak picking. Peak picking was performed independently for areas CA1 and CA3 and independently for OR and OLR paradigms. A static window with an iRT width of 6 min and a linear iRT calibration was used. For transition identification, a dynamic score refinement was used and the base entity was processed within the experiment. Decoys were generated using a scrambled, label-free decoy method. A normal distribution estimator was used for q-values. For transition quantification, an interference correction was used and the total peak area was used as normalization base.

SWATH-MS Data Normalization

SWATH-MS data were normalized with a custom script (Supplemental Experimental Procedures). Since large changes in time-dependent intensity were observed over different MS runs, a time-dependent normalization approach was used. Transitions were divided into 15 time windows according to their predicted iRT values. Time windows were normalized independently by summing up all intensities within MS runs and calculating a normalization factor matrix for all MS runs and time windows. Intensities for all transitions were then multiplied with the corresponding normalization factor.

Data Analyses

Following normalization, other scripts (Supplemental Experimental Procedures) were used to assign group and condition to each run and have a q-value cutoff over the experiments. Transitions for individual samples with a q-value > 0.01 and transitions for all samples with a q-value > 0.01 in more than 25% of samples were excluded. Further, proteins quantified with less than 2 peptides after q-value cutoff were excluded. Duplicate protein entries were removed before running any statistical analysis. Significance of the protein expression changes was assessed using MSstats (Choi et al., 2014), a proteomic tool using an R interface for statistical analysis of proteomic data on the transition level. MSstats performs an ANOVA over the whole dataset followed by two-group comparisons using unpaired t tests. A Benjamini-Hochberg approach was used for multiple testing corrections. Analyses were performed independently for areas CA1 and CA3 and for OR and OLR paradigms. Group comparisons between areas CA1 and CA3 in basal conditions and group comparisons between control-test pairs for every time point were performed.

Unsupervised Clustering

Unsupervised clustering was performed using R studio (v. 0.99.489) and the heatmap.2 function of the gplots package. First, intensity values of peptides were determined by summing up all transitions, and then intensity values of proteins were determined by summing up the normalized intensities of all peptides. Dendrograms for both row and column were computed and reordered.

Statistical Clustering of Fold Change

STEM software (v.1.3.8) (Ernst and Bar-Joseph, 2006) was used for statistical clustering of fold change values over time. For each combination of paradigm and subregion, a text file was prepared containing all protein IDs (significant and non-significant) with log2 fold change values of control-test comparison at each of the 4 time points. No normalization was performed with STEM software and a default STEM clustering method was used. 200 model profiles were generated with a maximum unit change in model profiles between time points of 2. The minimum absolute expression change was set to 0.2 for maximum-minimum. For all other parameters, default values were used.

Functional Annotation of Statistical Clusters

For each significant cluster, a list of Swiss-Prot accessions was extracted. The web-based gene set analysis toolkit (Zhang et al., 2005) (http://webgestalt.org) was used for functional annotation. An overrepresentation enrichment analysis was performed for cellular component using a non-redundant functional database. The protein list of each cluster was uploaded together with a list containing background identifiers from the same experiment. A GO analysis was performed using a hypergeometric statistical method with a Benjamini-Hochberg (BH) adjustment for multiple testing. The minimum number of genes for a category was set to 3.

DATA AND SOFTWARE AVAILABILITY

The accession number for the data reported in this paper is ProteomeXchange: PXD006382.

SUPPLEMENTAL INFORMATION

Supplemental Information includes Supplemental Experimental Procedures, six figures, and five tables and can be found with this article online at https://doi.org/10.1016/j.celrep.2018.02.079.

ACKNOWLEDGMENTS

This work was supported by the University of Zurich, the Swiss Federal Institute of Technology, the Swiss National Science Foundation (grant Nr 31003A_153147/1), and the Functional Genomics Center Zürich. We thank Professor Ralph Schlapbach for the scientific coordination at FGCZ; Asa Wahlander, Bernd Roschitzki, Christian Trachsel, and Claudia Fortes for technical assistance; Jonas Grossmann and Christian Panse for IT assistance; and Alexis Saucy for help with validations. Further, we thank Professor Angelika Steger and Professor Rudolf Aebersold for conceptual help and constructive discussions.

AUTHOR CONTRIBUTIONS

I.M.M. and L.M.v.Z. conceived the project and wrote the manuscript. L.M.v.Z. performed experiments and analyzed the data. N.S. contributed technical and theoretical expertise for proteomic measurements and data analyses. E.K. and R.Y.T.-C. performed some behavioral experiments.

DECLARATION OF INTERESTS

The authors declare no competing interests.

Received: May 25, 2017
Revised: January 5, 2018
Accepted: February 21, 2018
Published: March 20, 2018

REFERENCES

Anderse, P., Morris, R., and Amaral, D. (2006). The Hippocampus Book (Oxford Neuroscience).

Borger, E., Herrmann, A., Mann, D.A., Spires-Jones, T., and Gunn-Moore, F. (2014). The calcium-binding protein EFhd2 modulates synapse formation in vitro and is linked to human dementia. J. Neuropathol. Exp. Neurol. *73*, 1166–1182.

Borovok, N., Nesher, E., Levin, Y., Reichenstein, M., Pinhasov, A., and Michaelevski, I. (2016). Dynamics of Hippocampal Protein Expression During Long-term Spatial Memory Formation. Mol. Cell. Proteomics *15*, 523–541.

Broadbent, N.J., Gaskin, S., Squire, L.R., and Clark, R.E. (2009). Object recognition memory and the rodent hippocampus. Learn. Mem. *17*, 5–11.

Brown, M.W., Warburton, E.C., and Aggleton, J.P. (2010). Recognition memory: material, processes, and substrates. Hippocampus *20*, 1228–1244.

Buwalda, B., Kole, M.H., Veenema, A.H., Huininga, M., de Boer, S.F., Korte, S.M., and Koolhaas, J.M. (2005). Long-term effects of social stress on brain and behavior: a focus on hippocampal functioning. Neurosci. Biobehav. Rev. *29*, 83–97.

Cai, D.J., Aharoni, D., Shuman, T., Shobe, J., Biane, J., Song, W., Wei, B., Veshkini, M., La-Vu, M., Lou, J., et al. (2016). A shared neural ensemble links distinct contextual memories encoded close in time. Nature *534*, 115–118.

Cajigas, I.J., Will, T., and Schuman, E.M. (2010). Protein homeostasis and synaptic plasticity. EMBO J. *29*, 2746–2752.

Choi, M., Chang, C.Y., Clough, T., Broudy, D., Killeen, T., MacLean, B., and Vitek, O. (2014). MSstats: an R package for statistical analysis of quantitative mass spectrometry-based proteomic experiments. Bioinformatics *30*, 2524–2526.

Cohen, S.J., and Stackman, R.W., Jr. (2015). Assessing rodent hippocampal involvement in the novel object recognition task. A review. Behav. Brain Res. *285*, 105–117.

Csicsvari, J., O'Neill, J., Allen, K., and Senior, T. (2007). Place-selective firing contributes to the reverse-order reactivation of CA1 pyramidal cells during sharp waves in open-field exploration. Eur. J. Neurosci. *26*, 704–716.

Eichenbaum, H. (2004). Hippocampus: cognitive processes and neural representations that underlie declarative memory. Neuron *44*, 109–120.

Ernst, J., and Bar-Joseph, Z. (2006). STEM: a tool for the analysis of short time series gene expression data. BMC Bioinformatics *7*, 191.

Franz, A., Kevei, É., and Hoppe, T. (2015). Double-edged alliance: mitochondrial surveillance by the UPS and autophagy. Curr. Opin. Cell Biol. *37*, 18–27.

Frey, D., Laux, T., Xu, L., Schneider, C., and Caroni, P. (2000). Shared and unique roles of CAP23 and GAP43 in actin regulation, neurite outgrowth, and anatomical plasticity. J. Cell Biol. *149*, 1443–1454.

Gil, O.D., Zanazzi, G., Struyk, A.F., and Salzer, J.L. (1998). Neurotrimin mediates bifunctional effects on neurite outgrowth via homophilic and heterophilic interactions. J. Neurosci. *18*, 9312–9325.

Gilbert, P.E., Kesner, R.P., and Lee, I. (2001). Dissociating hippocampal subregions: double dissociation between dentate gyrus and CA1. Hippocampus *11*, 626–636.

Gillet, L.C., Navarro, P., Tate, S., Röst, H., Selevsek, N., Reiter, L., Bonner, R., and Aebersold, R. (2012). Targeted data extraction of the MS/MS spectra generated by data-independent acquisition: a new concept for consistent and accurate proteome analysis. Mol. Cell. Proteomics *11*, O111.016717.

Girouard, H., Wang, G., Gallo, E.F., Anrather, J., Zhou, P., Pickel, V.M., and Iadecola, C. (2009). NMDA receptor activation increases free radical production through nitric oxide and NOX2. J. Neurosci. *29*, 2545–2552.

Goeldner, C., Ballard, T.M., Knoflach, F., Wichmann, J., Gatti, S., and Umbricht, D. (2013). Cognitive impairment in major depression and the mGlu2 receptor as a therapeutic target. Neuropharmacology *64*, 337–346.

Gunasekar, P.G., Kanthasamy, A.G., Borowitz, J.L., and Isom, G.E. (1995). NMDA receptor activation produces concurrent generation of nitric oxide and reactive oxygen species: implication for cell death. J. Neurochem. *65*, 2016–2021.

Guzowski, J.F., Knierim, J.J., and Moser, E.I. (2004). Ensemble dynamics of hippocampal regions CA3 and CA1. Neuron *44*, 581–584.

Heckers, S., and Konradi, C. (2010). Hippocampal pathology in schizophrenia. Curr. Top. Behav. Neurosci. *4*, 529–553.

Hoge, J., and Kesner, R.P. (2007). Role of CA3 and CA1 subregions of the dorsal hippocampus on temporal processing of objects. Neurobiol. Learn. Mem. *88*, 225–231.

Hu, X.L., Wang, Y., and Shen, Q. (2012). Epigenetic control on cell fate choice in neural stem cells. Protein Cell *3*, 278–290.

Huang, C.W., Huang, C.C., Cheng, J.T., Tsai, J.J., and Wu, S.N. (2007). Glucose and hippocampal neuronal excitability: role of ATP-sensitive potassium channels. J. Neurosci. Res. *85*, 1468–1477.

Huerta, P.T., Sun, L.D., Wilson, M.A., and Tonegawa, S. (2000). Formation of temporal memory requires NMDA receptors within CA1 pyramidal neurons. Neuron *25*, 473–480.

Hunsaker, M.R., Lee, B., and Kesner, R.P. (2008). Evaluating the temporal context of episodic memory: the role of CA3 and CA1. Behav. Brain Res. *188*, 310–315.

Kaczorowski, C.C., and Disterhoft, J.F. (2009). Memory deficits are associated with impaired ability to modulate neuronal excitability in middle-aged mice. Learn. Mem. *16*, 362–366.

Karlsson, M.P., and Frank, L.M. (2008). Network dynamics underlying the formation of sparse, informative representations in the hippocampus. J. Neurosci. *28*, 14271–14281.

Kesner, R.P., Hunsaker, M.R., and Ziegler, W. (2010). The role of the dorsal CA1 and ventral CA1 in memory for the temporal order of a sequence of odors. Neurobiol. Learn. Mem. *93*, 111–116.

Knaus, P., Marquèze-Pouey, B., Scherer, H., and Betz, H. (1990). Synaptoporin, a novel putative channel protein of synaptic vesicles. Neuron *5*, 453–462.

Knierim, J.J., Lee, I., and Hargreaves, E.L. (2006). Hippocampal place cells: parallel input streams, subregional processing, and implications for episodic memory. Hippocampus *16*, 755–764.

Köster, J.D., Leggewie, B., Blechner, C., Brandt, N., Fester, L., Rune, G., Schweizer, M., Kindler, S., and Windhorst, S. (2016). Inositol-1,4,5-trisphosphate-3-kinase-A controls morphology of hippocampal dendritic spines. Cell. Signal. *28*, 83–90.

Lambert, A.J., and Brand, M.D. (2009). Reactive oxygen species production by mitochondria. Methods Mol. Biol. *554*, 165–181.

Larkin, M.C., Lykken, C., Tye, L.D., Wickelgren, J.G., and Frank, L.M. (2014). Hippocampal output area CA1 broadcasts a generalized novelty signal during an object-place recognition task. Hippocampus *24*, 773–783.

Lee, I., Hunsaker, M.R., and Kesner, R.P. (2005). The role of hippocampal subregions in detecting spatial novelty. Behav. Neurosci. *119*, 145–153.

Lehmann, G., Udasin, R.G., and Ciechanover, A. (2016). On the linkage between the ubiquitin-proteasome system and the mitochondria. Biochem. Biophys. Res. Commun. *473*, 80–86.

Leutgeb, S., Leutgeb, J.K., Treves, A., Moser, M.B., and Moser, E.I. (2004). Distinct ensemble codes in hippocampal areas CA3 and CA1. Science *305*, 1295–1298.

Lisman, J.E., and Otmakhova, N.A. (2001). Storage, recall, and novelty detection of sequences by the hippocampus: elaborating on the SOCRATIC model to account for normal and aberrant effects of dopamine. Hippocampus *11*, 551–568.

Maruszak, A., and Żekanowski, C. (2011). Mitochondrial dysfunction and Alzheimer's disease. Prog. Neuropsychopharmacol. Biol. Psychiatry *35*, 320–330.

McKay, B.M., Matthews, E.A., Oliveira, F.A., and Disterhoft, J.F. (2009). Intrinsic neuronal excitability is reversibly altered by a single experience in fear conditioning. J. Neurophysiol. *102*, 2763–2770.

Molfese, D.L. (2011). Advancing neuroscience through epigenetics: molecular mechanisms of learning and memory. Dev. Neuropsychol. *36*, 810–827.

Monopoli, M.P., Raghnaill, M.N., Loscher, J.S., O'Sullivan, N.C., Pangalos, M.N., Ring, R.H., von Schack, D., Dunn, M.J., Regan, C.M., Pennington, S., and Murphy, K.J. (2011). Temporal proteomic profile of memory consolidation in the rat hippocampal dentate gyrus. Proteomics *11*, 4189–4201.

Moser, E.I., Kropff, E., and Moser, M.B. (2008). Place cells, grid cells, and the brain's spatial representation system. Annu. Rev. Neurosci. *31*, 69–89.

Moyer, J.R., Jr., Thompson, L.T., and Disterhoft, J.F. (1996). Trace eyeblink conditioning increases CA1 excitability in a transient and learning-specific manner. J. Neurosci. *16*, 5536–5546.

Nandi, D., Tahiliani, P., Kumar, A., and Chandu, D. (2006). The ubiquitin-proteasome system. J. Biosci. *31*, 137–155.

Navarro, A., and Boveris, A. (2010). Brain mitochondrial dysfunction in aging, neurodegeneration, and Parkinson's disease. Front. Aging Neurosci. *2*, 34.

Navarro, A., López-Cepero, J.M., Bández, M.J., Sánchez-Pino, M.J., Gómez, C., Cadenas, E., and Boveris, A. (2008). Hippocampal mitochondrial dysfunction in rat aging. Am. J. Physiol. Regul. Integr. Comp. Physiol. *294*, R501–R509.

Newrzella, D., Pahlavan, P.S., Krüger, C., Boehm, C., Sorgenfrei, O., Schröck, H., Eisenhardt, G., Bischoff, N., Vogt, G., Wafzig, O., et al. (2007). The functional genome of CA1 and CA3 neurons under native conditions and in response to ischemia. BMC Genomics *8*, 370.

Nitz, D., and McNaughton, B. (2004). Differential modulation of CA1 and dentate gyrus interneurons during exploration of novel environments. J. Neurophysiol. *91*, 863–872.

Oh, M.M., Oliveira, F.A., and Disterhoft, J.F. (2010). Learning and aging related changes in intrinsic neuronal excitability. Front. Aging Neurosci. *2*, 2.

Oh, M.M., Simkin, D., and Disterhoft, J.F. (2016). Intrinsic Hippocampal Excitability Changes of Opposite Signs and Different Origins in CA1 and CA3 Pyramidal Neurons Underlie Aging-Related Cognitive Deficits. Front. Syst. Neurosci. *10*, 52.

Oliveira-da-Silva, A., Vieira, F.B., Cristina-Rodrigues, F., Filgueiras, C.C., Manhães, A.C., and Abreu-Villaça, Y. (2009). Increased apoptosis and reduced neuronal and glial densities in the hippocampus due to nicotine and ethanol exposure in adolescent mice. Int. J. Dev. Neurosci. *27*, 539–548.

Rajji, T., Chapman, D., Eichenbaum, H., and Greene, R. (2006). The role of CA3 hippocampal NMDA receptors in paired associate learning. J. Neurosci. *26*, 908–915.

Rao-Ruiz, P., Carney, K.E., Pandya, N., van der Loo, R.J., Verheijen, M.H., van Nierop, P., Smit, A.B., and Spijker, S. (2015). Time-dependent changes in the mouse hippocampal synaptic membrane proteome after contextual fear conditioning. Hippocampus *25*, 1250–1261.

Solaini, G., Baracca, A., Lenaz, G., and Sgarbi, G. (2010). Hypoxia and mitochondrial oxidative metabolism. Biochim. Biophys. Acta *1797*, 1171–1177.

Squire, L.R. (2006). Lost forever or temporarily misplaced? The long debate about the nature of memory impairment. Learn. Mem. *13*, 522–529.

Tobe, E.H. (2013). Mitochondrial dysfunction, oxidative stress, and major depressive disorder. Neuropsychiatr. Dis. Treat. *9*, 567–573.

VanElzakker, M., Fevurly, R.D., Breindel, T., and Spencer, R.L. (2008). Environmental novelty is associated with a selective increase in Fos expression in the output elements of the hippocampal formation and the perirhinal cortex. Learn. Mem. *15*, 899–908.

Vann, S.D., and Albasser, M.M. (2011). Hippocampus and neocortex: recognition and spatial memory. Curr. Opin. Neurobiol. *21*, 440–445.

Wilson, M.A., and McNaughton, B.L. (1993). Dynamics of the hippocampal ensemble code for space. Science *261*, 1055–1058.

Winklhofer, K.F., and Haass, C. (2010). Mitochondrial dysfunction in Parkinson's disease. Biochim. Biophys. Acta *1802*, 29–44.

Wiśniewski, J.R., Zougman, A., Nagaraj, N., and Mann, M. (2009). Universal sample preparation method for proteome analysis. Nat. Methods *6*, 359–362.

Yang, G., Pan, F., and Gan, W.B. (2009). Stably maintained dendritic spines are associated with lifelong memories. Nature *462*, 920–924.

Yonelinas, A.P., Kroll, N.E., Quamme, J.R., Lazzara, M.M., Sauvé, M.J., Widaman, K.F., and Knight, R.T. (2002). Effects of extensive temporal lobe damage or mild hypoxia on recollection and familiarity. Nat. Neurosci. *5*, 1236–1241.

Zhang, B., Kirov, S., and Snoddy, J. (2005). WebGestalt: an integrated system for exploring gene sets in various biological contexts. Nucleic Acids Res. *33*, W741–W748.

Zhang, L., Zhou, R., Li, X., Ursano, R.J., and Li, H. (2006). Stress-induced change of mitochondria membrane potential regulated by genomic and non-genomic GR signaling: a possible mechanism for hippocampus atrophy in PTSD. Med. Hypotheses *66*, 1205–1208.

Zhu, X.H., Qiao, H., Du, F., Xiong, Q., Liu, X., Zhang, X., Ugurbil, K., and Chen, W. (2012). Quantitative imaging of energy expenditure in human brain. Neuroimage *60*, 2107–2117.